Journal of Non-Crystalline Solids 570 (2021) 121006

Contents lists available at ScienceDirect

Journal of Non-Crystalline Solids

journal homepage: www.elsevier.com/locate/jnoncrysol

Amorphous boron phosphide: An ab initio investigation

Süleyman Bolat [a], Murat Durandurdu [b,c,*]

[a] Faculty of Science, Department of Physics, Karadeniz Technical University, Trabzon, 61080, Turkey
[b] Department of Physical and Macromolecular Chemistry, Charles University, Prague, 12843, Czech Republic
[c] Nanotechnology Engineering, Abdullah Gül University, Kayseri, 38080, Turkey

ARTICLE INFO

Keywords:
Amorphous
Boron phosphide
Chemical disorder
Ab initio

ABSTRACT

We generate a structural model of amorphous boron phosphide (BP) by quenching the melt via ab initio molecular dynamics calculations and compare it structurally and electrically with the crystal. We find that both phases of BP have a significantly different short-range order. Namely, the amorphous network presents strong chemical disorder and structural defects. P-atoms form only undercoordinated defects while B atoms present both undercoordinated and overcoordinated defects. The mean coordination number of B and P atoms is 4.17 and 3.69, correspondingly. Some of overcoordinated B atoms with chemical disorder yield the formation of pentagonal-pyramid-like motifs and a cage-like B_{10} cluster in the amorphous network. About 13 % volume expansion is observed by amorphization, probably due to the low-coordinated structural defects. The amorphous configuration is semiconductor as in the crystal but has a smaller energy band gap.

1. Introduction

Boron phosphide (BP), a member of the III-V semiconductor families, was first synthesized in 1957 [1]. It has the zinc blende (ZB) structure having a lattice parameter of 4.55 Å. BP has remarkable properties such as high thermal conductivity [2,3], high chemical inertness, high hardness [4–6], a high melting point [3,7] and a wide band gap [8–10]. Therefore it can be used in electronic-optic devices, neutron detectors, high temperature applications and intense radiation applications [11–15].

In spite of its remarkable properties, the studies on this material are limited due the complications in the growing of single crystals [13,16]. In some investigations, depending on the preparation techniques and/or conditions, partially or fully amorphized BP samples were detected [5,7, 17–19]. However, no serious attention has been paid to understand the structure and properties of amorphous BP form so far. It was only argued that its chemical properties are considerably different from those of the ZB crystal [5]. Here we carry out ab initio molecular dynamics (AIMD) simulations to shed some light on the microstructure and the electrical behavior of amorphous BP. An amorphous BP model is achieved using the rapid solidification of the melt and found to be structurally and electronically different than the crystal, consisting with the experimental prediction [5].

2. Methodology

The SIESTA ab initio software [20] was used with the Martins-Troullier pseudopotential method [21] and Lee-Yang-Parr (LYP) GGA approximation [22,23] to investigate BP phases. We selected the double-zeta (DZ) basis for AIMD simulations and the double-zeta plus polarized (DZP) basis for the structural optimization. The Brillion zone integration was performed at the Γ point. The NPT methodology was chosen to accomplish AIMD simulations having 1.0 fs for each time step. Pressure was controlled by the Parrinello-Rahman method [24] whose fictitious mass was set to be 20.0 Ry.fs^2. Temperature was controlled by the velocity scaling method. We used two starting structures having 216 atoms, different density, local structure and chemical environments. The first structure, referred as model 1, was the cubic ZB crystal. It is chemically ordered and has perfect fourfold coordination. Its optimized volume using DZP basis is 12.28 Å^3/atom (corresponding the lattice parameter is 4.61 Å, comparable with the experimental result of 4.55 Å [1]). The second structure, referred as model 2, was an amorphous boron arsenide (BAs) model [25]. It is chemically disordered and the mean coordination number of B- and As-atoms is 4.97 and 3.34, correspondingly. Its volume is 19.49 Å^3/atom. These two initial structures were melted at 4000 K for 5.0 ps, well above the experimental melting temperature of about 1400 K. At 4000 K, the pressure applied was set to be 5 GPa in order to

* Corresponding author.
E-mail address: murat.durandurdu@agu.edu.tr (M. Durandurdu).

https://doi.org/10.1016/j.jnoncrysol.2021.121006
Received 7 April 2021; Received in revised form 29 May 2021; Accepted 15 June 2021
Available online 28 June 2021

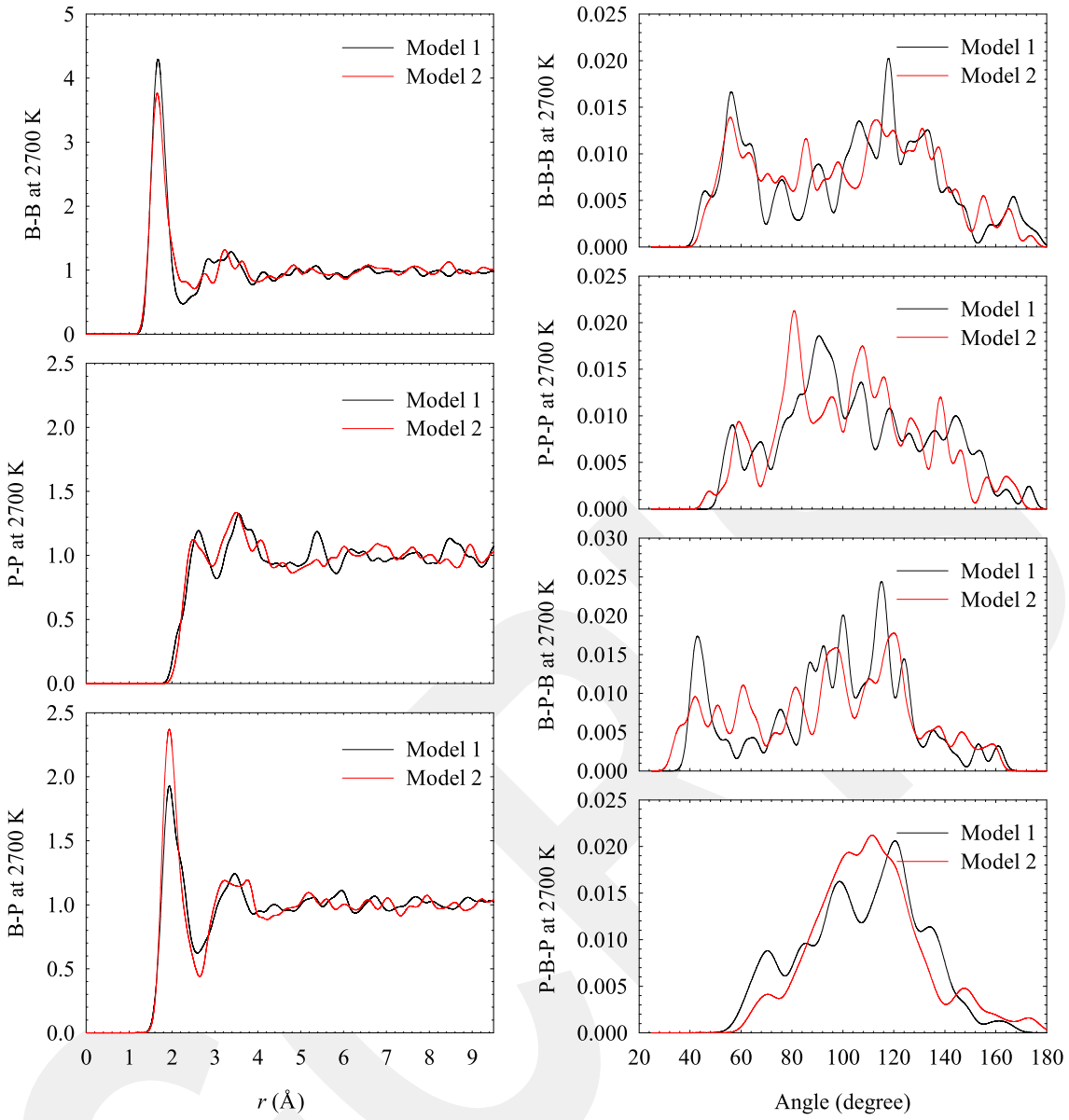

Fig. 1. Pair distribution functions (PDFs) and bond angle distribution functions (BADFs) of model 1 and model 2 at 2700 K. The statical average of 1000 MD steps is used for the structural analysis.

eliminate a drastic volume expansion due to a sudden high temperature application. Then the melts were quenched to 2700 K in 10.0 ps. At this temperature, pressure was set to be 0.5 GPa and the structures were thermalized for 40 ps. After that, an additional 1000 MD steps were run to collect data for the structural investigations. The equilibrated configurations at 2700 K were analyzed using the pair correlation functions and angles distribution functions, which are provided in Fig. 1. The structural analyses expose that both networks have *almost* the same local environment and volume. The volume of model 1 and model 2 at this temperature was found to be 18.98 $Å^3$/atom and 19.01 $Å^3$/atom, respectively. All these findings suggest that our simulation time was long enough to have an equilibrium melt and volume for BP. Therefore, in order to reduce the computational efforts, we chosen model 2 to generate an amorphous BP network because it presented slightly less chemical disorder than model 1. For model 2, the applied temperature was gradually decreased to 300 K using a cooling rate of 1.0×10^{13} K/s. The resultant structure at room temperature was relaxed using the DZP basis and a variable-cell conjugate-gradient optimization technique till the maximum atomic force was smaller than 0.01 eV/Å. The relative energy difference between the amorphous and crystal structures is computed to be about 0.46 eV/atom. The volume of the relaxed amorphous BP configuration is 13.95 $Å^3$/atom.

3. Results

Fig. 2 compares the B-B, P-P and B-P pair correlations of the computer-generated amorphous model with those of the ZB-crystal and reveals the radical distinctions between the amorphous configuration and the crystal. Namely, one can see the formation of B-B and P-P homopolar bonds as indicted by the peak at 1.75 Å and 2.29 Å, respectively, in the amorphous network. Accordingly, the amorphous network shows strong chemical disorder. The B-B bond length (1.75 Å) seems to be significantly shorter than 1.80 Å in amorphous B [26], 1.802 (1.803 Å) in α- (β-) rhombohedral B crystals [27] and 1.76 Å in liquid B [28]. This is possibly associated with the coordination number of B atom such that it is less in the amorphous BP model than in the other forms of

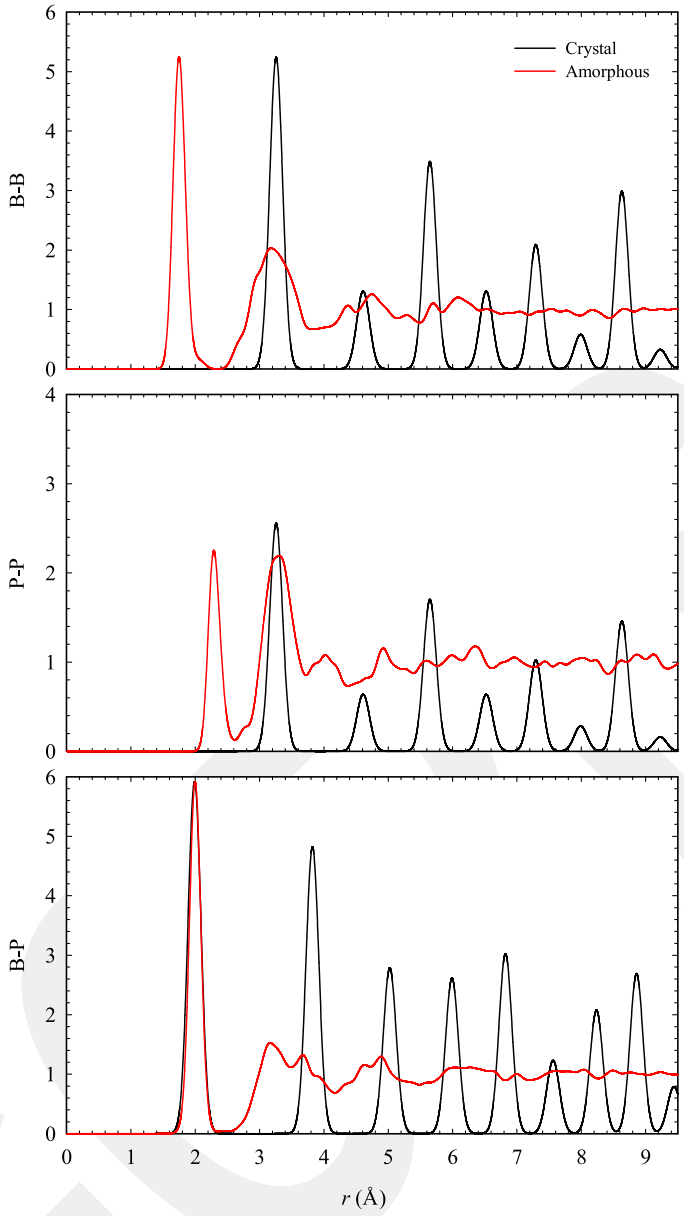

Fig. 2. Pair distribution functions (PDFs) of the amorphous and crystalline BP. The peak intensity of the crystal structure was scaled to the peak intensity value of amorphous structure for clarity.

B. The peak of P-P bonds is located at 2.29 Å, which is slightly longer than 2.13-2.27 Å in the crystalline or amorphous P phases having threefold coordination [29–31]. The B-P bond separation of the amorphous configuration is positioned at 2.00 Å, in good agreement with 1.99 Å estimated for the ZB crystal. Our crystal value is reasonably parallel to the experimental result of 1.965 Å [8] but slightly longer than the theoretical value found as 1.906 Å [32,33].

The coordination number and distribution obtained using the first minimum of the pair correlations (2.34 Å for B-B, 2.61 Å for P-P and 2.35 Å for B-P) can deliver crucial information about the short-range order of noncrystalline BP. As seen from Fig.3, the coordination of B atoms varies from three to six. The fourfold coordination with a fraction of 67.6% is the most dominant one followed by threefold coordination with a frequency of 13%. The amorphous network has also fivefold and sixfold coordination (9.3% and 10.2%, respectively) and some of which procedure ideal or imperfect pentagonal pyramid-like configurations, the main unit of the B_{12} icosahedron. For B-atom, B-B, B-P and total coordination numbers are about 1.78, 2.39 and 4.17, respectively. On the other hand, P atoms form only threefold and fourfold coordinated motifs having a fraction of 31.5% and 68.5%, correspondingly. For P atom, P-P, P-B and total coordination are, respectively, about 1.30, 2.39 and 3.69. From these results, four important conclusions can be drawn: (*i*) B atoms form more homopolar bonds than P atoms, (*ii*) both species have almost an equal number of tetragonal coordination (*iii*) B atoms have both undercoordinated and overcoordinated defects while P atoms have only undercoordinated defects, (*iv*) the total coordination number of P and B noticeably diverges from fourfold coordination.

The chemical environment of B and P atoms provided in Table 1 can offer more knowledge about the amorphous structure at the atomistic level. The crystal is chemically ordered and hence it has only B-P_4 and P-B_4 units. These units do indeed exist in the amorphous model as well but their fraction is about 17.6%. For B-atoms, the different types of

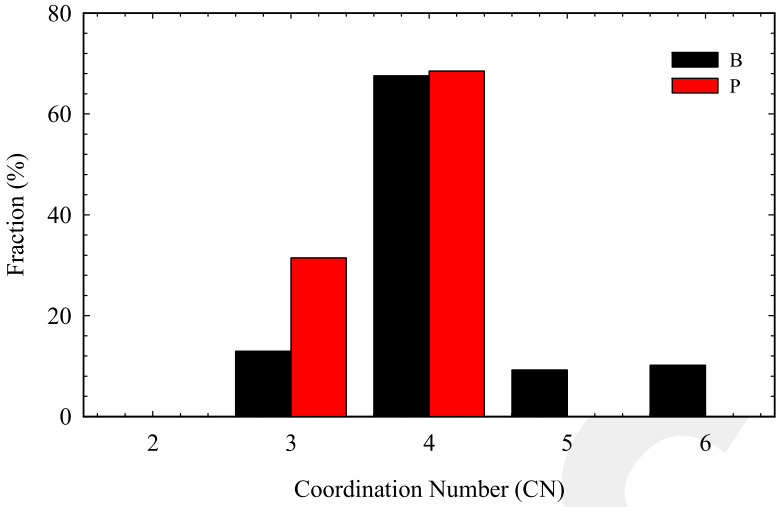

Fig. 3. The coordination distribution of B and P atoms.

structural arrangements such as B-BP_3, B-BP_2, B-B_2P_2 and B-B_2P emerge in the amorphous configuration as seen from the Table 1. B-BP_3 is the most preferred one with a rate of 36% followed by B-B_4 (17.6%), B-B_2P_2 (10%), B-B_2P (7.4%) and B-B_5P (6.5%). For P atoms, on the other hand, P-B_3P (25%), P-B_2P_2 (20.4%), P-B_4 (17.6%), P-B_2P (10.2%) and P-BP_2 (10.2%) types of configurations are the most common ones. These results reveal the fact that amorphous and crystalline phases of BP have a considerably diverse chemical environment for each species, in agreement with experimental prediction [5] and the amorphous structure presents robust chemical disorder such that about 82 % of P and B atoms involve wrong bond(s), between like atoms.

Some examples of bond angle distribution functions (BADFs) of the disordered network are illustrated in Fig. 4. The ordered structure has the P-B-P and B-P-B angles at ~109.5°. In the amorphous configuration, on the other hand, due to the chemical disorder, different types of angle distributions are presented. The P-B-P bonds lead to a peak at around 109.3°, close to the tetrahedral angle of 109.5°. On the other hand, the B-P-B distribution has a broad peak near 110°. The weak peak at ~54° is due to the threefold ring, a part of a pentagonal pyramid-like motif. The B-B-B distribution has peaks at around 60° and 107°, similar to amorphous B, which are produced by pentagonal-like configurations formed in the amorphous model (see Fig. 5). Due to the formation of different kinds of P-P-P chain-like structures in the amorphous network (see Fig. 5), the P-P-P bonds produce a wide distribution but a sharp peak at around 100°, close to 99° in black phosphorus having zigzag chains of P atoms. The angle distribution analysis indicates the presence of some traces of the tetrahedral character in the amorphous network.

Table 1
Fraction of the chemical environment around B and P atoms in amorphous BP.

B		P	
BP_2	3.704	BP_2	10.185
BP_3	36.111	BP_3	5.556
B_2P	7.407	B_2P	10.185
B_2P_2	10.185	B_2P_2	20.370
B_3P	3.704	B_3	5.556
B_3P_2	1.852	B_3P	25.000
B_4	17.593	B_4	17.593
B_4P	5.556	P_3	5.556
B_5	1.852		
B_5P	6.481		
B_6	3.704		
P_3	1.852		

Finally, the total and partial electron density of states (DOS) of the amorphous and crystalline BP structures are calculated and given in Fig. 6. The forbidden energy gap energy of the crystal structure is determined as 1.70 eV, smaller than the experimental value of about 2.00 eV [34,35] as expected due to the restraint of DFT calculations but it is higher than the previous theoretical data of 1.11-1.38 eV [11, 36–49] estimated using different exchange functionals. For the amorphous phase, due to the smoothing factor of 0.20 eV, the DOS exhibits a typical feature of a semimetallic material, i.e., no clear band gap but it has a band gap of 0.46 eV. So amorphization results in a noticeable decrease in the band gap of BP. Considering about 15 % underestimation of the band gap energy in the crystal, we can speculate that it could be ~0.54 eV for the amorphous BP model. Yet we should note here that experimental study suggested that the amorphous film with the ratio of B:P ~ 1 has a band gap of 2.04 eV [17], quite larger than our prediction.

The partial DOS can provide detailed and specific information about the electronic structure of these systems. As can be seen form Fig. 5, P-*p* and B-*p* states provide the core influence to both valence and conduction bands near the Fermi level (at zero eV).

In order to better understand the electronic structure of the amorphous model we also estimate the inverse participation ratio (IPR)

$$\mathrm{IPR}(\psi_j) = N\sum_{i=1}^{N} a_i^{m4} \Big/ \left(\sum_{i=1}^{N} a_i^{m2}\right)^2$$

where $\psi_m = \sum_{i=1}^{N} a_i^m \phi_i$ is the m^{th} eigenstate and N is the number of atoms (see Ref. [47]). The IPR calculated is illustrated in Fig. 7. It can be seen that the states near the Fermi level have high IPR, indicating a high localization. It should be note that the localization is seen in both conduction and valence band tail states and their IPR has almost the same intensity. The symmetry on IPR between valence and conduction band tails might indicate that both n-type and p-type doping can be suitable for amorphous BP.

4. Discussion

Our results expose that the short-range order and chemical properties of amorphous form of BP is considerably different than those of the crystalline counterpart, consisting with the experimental prediction [5]. The amorphous model exhibits noticeable coordination defects and strong chemical disorder such that about 82% of atoms involve homopolar bond(s). The formation of wrong bonds and coordination defects is energetically not favorable but commonly seen in nonionic amorphous

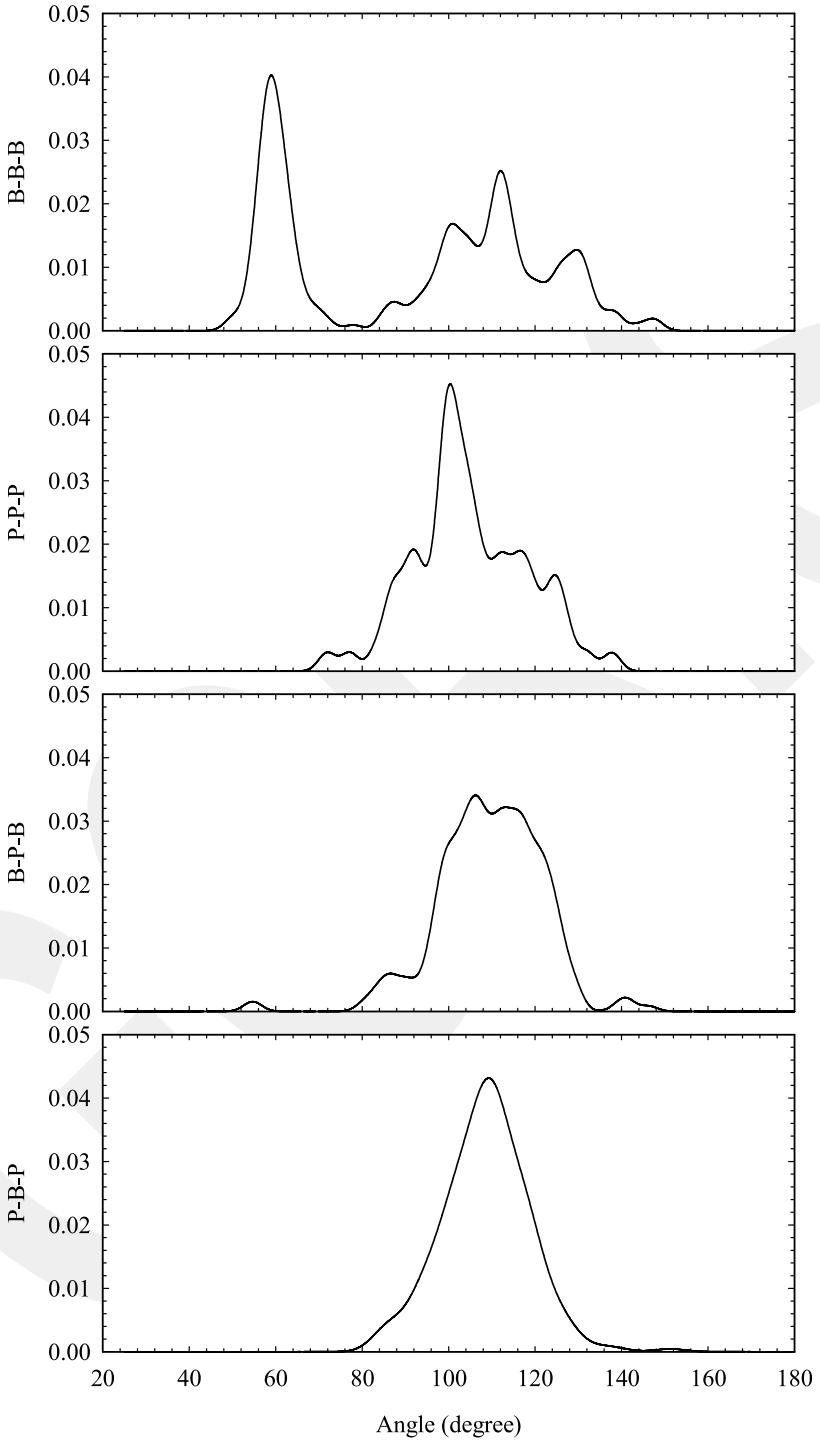

Fig. 4. Bond angle distribution functions (BADFs) of the amorphous BP configuration.

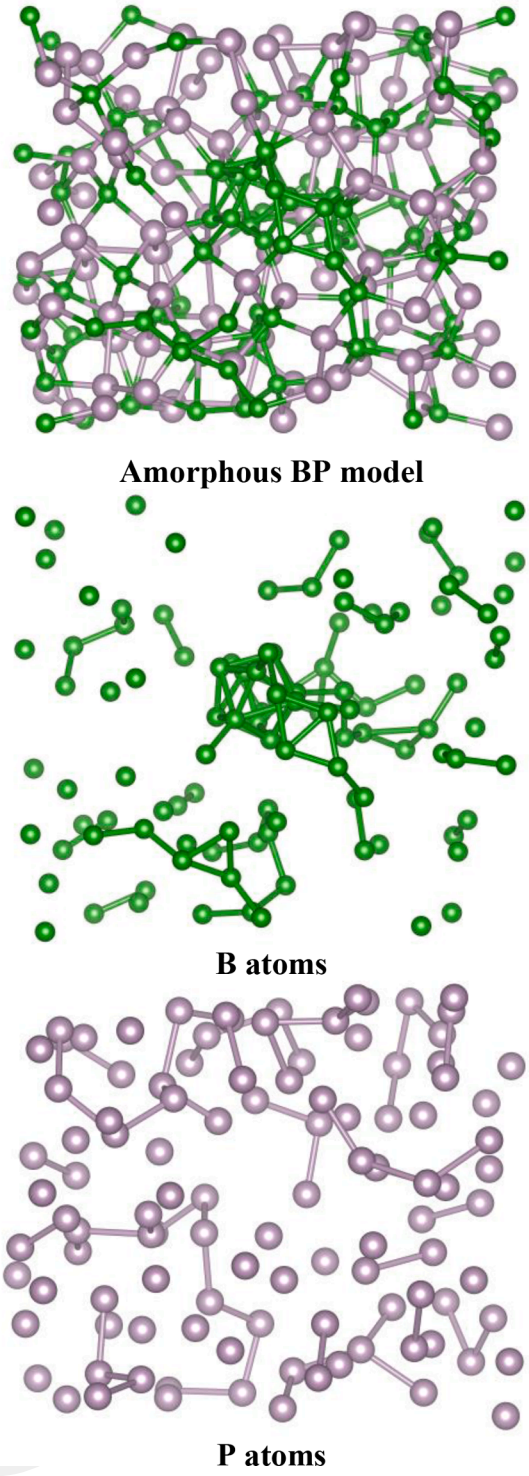

Fig. 5. Ball-stick demonstration of the amorphous model.

alloys such as gallium phosphide (GaP) [48], indium phosphide (InP) [49] and BAs [25]. The low ionicity of BP is likely the main reason for the observation of a large fraction of homopolar bonds in the amorphous network. The mean coordination of amorphous BP deviates from tetrahedral coordination. When the structural defects are considered, P atoms prefer to form only undercoordinated defects while B atoms form both undercoordinated and overcoordinated defects. The amorphous model is a solid solution but the P-P-P and B-B-B chain-like structures exist in the model. The overcoordinated motifs (sixfold and fivefold B-atoms) yield the formation of pentagonal-pyramid-like structures in the amorphous state, the key building unit of B_{12} icosahedra and B and B-rich materials. Yet a complete B_{12} icosahedron does not form in our amorphous configuration and instead a B_{10} cluster is observed. One might argue that the small size of simulation box and/or the time scale of simulation used in the present work might not allow the development of B_{12} molecule in the present work. This is certainly possible but we need to note here that B_{12} molecules are observed in a 200-atom model of amorphous boron silicide (BSi) generated even using a higher cooling

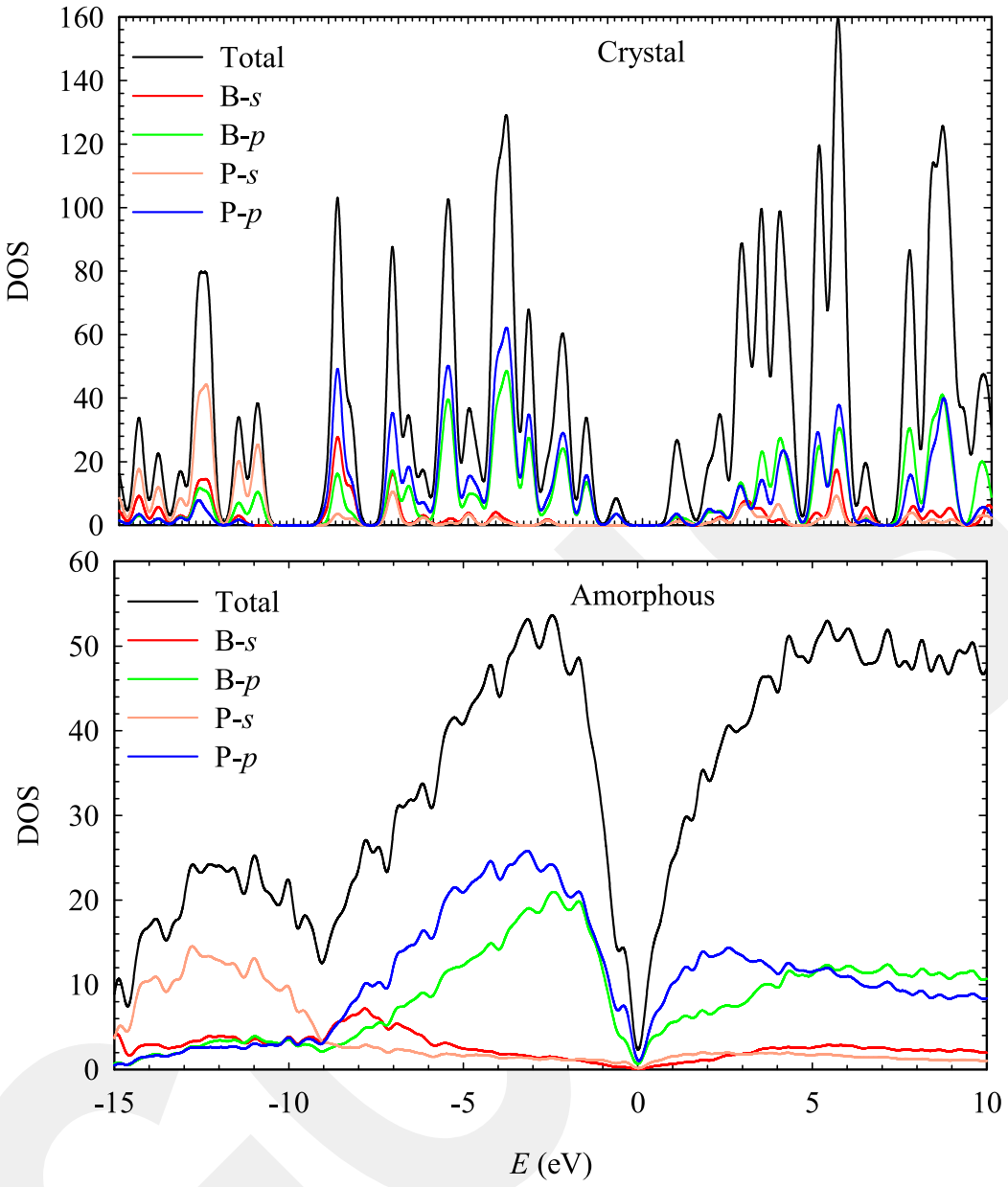

Fig. 6. Total and partial electron density of state (DOS) of the amorphous and crystalline BP phases.

rate. This finding weakens these two concerns. Nonetheless, generating larger models using a slower cooling rate might fully eliminate these concerns. Also, such investigations will be very useful in determining the effects of size and time scale of simulation on the amount of chemical and structural defects in amorphous BP.

A volume swelling is generally witnessed by amorphization. This is due to the structural disorder. In our amorphous BP model, we observe a quite large volume expansion about 13 % (the equilibrium volume of the amorphous and crystalline states is 13.95 Å^3/atom and 12.28 Å^3/atom, respectively). The open structured configurations, we believe that, are responsible for a large volume enlargement in amorphous BP.

The semiconducting nature of our model in spite of its large chemical disorder and structural defects, perhaps, is an interesting observation. According to our finding, amorphous BP can be classified as a narrow band gap semiconductor in a contrast to the crystal. This suggestion is, however, not consistent with the experimental work, recommending that amorphous BP has a band gap of about 2.0 eV and can serve as a wide gap semiconductor [17]. We should note here that the experimental sample with the ratio of B:P ∼ 1 presents B-H vibration mode indicating that the sample is not as pure as our model. So, the presence of H atoms and some other impurities might be a main factor for the observation of the discrepancy on the band gap energy since hydrogenation significantly affects the electronic structure of amorphous materials. Further experimental and computational investigations are needed to explore the influence of hydrogenation on the atomic and electronic structures of amorphous BP.

5. Conclusions

We have studied the atomic structure and the electrical character of an amorphous BP model generated using the melt-and-quench method via ab initio MD calculations and find that it is structurally and electrically different from the crystal. The model exhibits strong chemical disorder, which is probably because of the low ionicity of BP. Its coordination number deviates from the tetrahedral coordination. P atoms have a trend to form undercoordinated structural defects and P-P-P chain-like structures. On the other hand, B atoms form both undercoordinated and overcoordinated structural defects and chain-like and

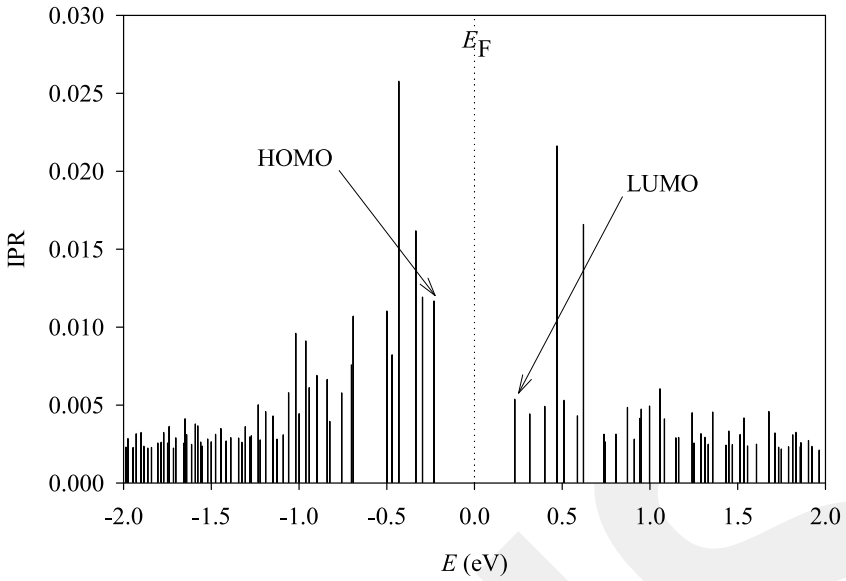

Fig. 7. Inverse participation ratio (IPR) estimated for the amorphous model.

pentagonal-pyramid-like configurations. We believe that the low coordinated configurations lead to a large volume enlargement (about 13%) in the amorphous form. In spite of large fraction of homopolar bonds and coordination defects, amorphous BP is found to be a semiconducting material and has a smaller band energy band gap than the crystal but its electronic structure can be sensitive to the experimental preparation techniques, impurities etc.. We should note here that all these conclusions are based on a 216-atom model. Further experimental studies are undoubtedly needed to clarify the short-range of amorphous BP and its properties.

CRediT authorship contribution statement

Süleyman Bolat: Data curation, Formal analysis, Investigation, Validation, Visualization, Writing - original draft. **Murat Durandurdu:** Conceptualization, Funding acquisition, Methodology, Resources, Supervision, Writing - review & editing.

Declaration of Competing Interest

The authors declare that they have no conflict of interest.

Acknowledgements

MD acknowledges financial support from the Abdullah Gül University Support Foundation.

The calculations were run on TÜBİTAK ULAKBİM, High Performance and Grid Computing Center (TRUBA resources).

References

[1] P. Popper, T.A. Ingles, Boron phosphide, a III-V compound of zinc-blende structure, Nature 179 (1957) 1075.
[2] A. Golikova, Boron and boron-based semiconductors, Phys. Status Solidi 51 (1979) 11–40.
[3] S. Tugo, T. Kipxura, Thermoelectric power of boron phosphide at high temperature, Phys. Status Solidi 59 (1980) 363–370.
[4] B. Stone, D. Hill, Semiconducting properties of cubic phosphide, Phys. Rev. Lett. 4 (1960) 282–284.
[5] F.V. Williams, R.A. Ruehrwein, The preparation and properties of boron phosphides and arsenides, Am. Chem. Soc. 82 (1960) 1330–1332.
[6] Y.Le Godec, M. Mezouar, O.O. Kurakevych, P. Munsch, U. Nwagwu, J.H. Edgar, V. L. Solozhenko, Equation of state of single-crystal cubic boron phosphide, J. Superhard Mater. 36 (2014) 61–64.
[7] Y. Kumasiro, T. Yokoyama, T. Sakamoto, T. Fujita, Preparation and electrical properties of boron and boron phosphide films obtained by gas source molecular beam deposition, J. Solid State Chem. 133 (1997) 269–272.
[8] C.C. Wang, M. Cardona, A.G. Fischer, Preparation, optical properties, and band structure of boron monophosphide, RCA Rev. 25 (1964) 159–167.
[9] R.I. Stearns, Band gap of boron phosphide, J. Appl. Phys. 36 (1965) 330–331.
[10] B. Bouhafs, H. Aourag, M. Certier, Trends in band-gap pressure coefficients in boron compounds BP, BAs, and BSb, J. Phys. Condens. Matter. 12 (2000) 5655–5668.
[11] S. Cui, W. Feng, H. Hu, Z. Feng, Y. Wang, First-principles study of zinc-blende to rocksalt phase transition in BP and BAs, Comput. Mater. Sci. 44 (2009) 1386–1389.
[12] T. Takenaka, M. Takigawa, K. Shohno, Diffusion layers formed in Si substrates during the epitaxial growth of BP and application to devices, J. Electrochem. Soc. 125 (1978) 633–637.
[13] Y. Kumashiro, Refractory semiconductor of boron phosphide, J. Mater. Res. 5 (1990) 2947–2983.
[14] J.C. Lund, F. Olschner, F. Ahmed, K.S. Shah, Boron phosğhide on silicon for radiation detectors, Mater. Res. Soc. 162 (1990) 601–604.
[15] T.P. Viles, B.A. Brunett, H. Yoon, J.C. Lund, H. Hermon, D. Buchenauer, K. Mccarty, M. Clifft, D. Dibble, R.B. James, Material requirements for a boron phosphide thermal neutron counter, Mater. Res. Soc. (1998) 585–590.
[16] V.A. Mukhanov, P.S. Sokolov, Y.Le Godec, V.L. Solozhenko, Self-propagating high-temperature synthesis of boron phosphide, J. Superhard Mater. 35 (2013) 415–417.
[17] S. Dalui, S. Hussain, S. Varma, D. Paramanik, A.K. Pal, Boron phosphide films prepared by co-evaporation technique: Synthesis and characterization, Thin Solid Films 516 (2008) 4958–4965.
[18] K. Woo, K. Lee, K. Kovnir, BP: Synthesis and properties of boron phosphide, Mater. Res. Express. 3 (2016) 074003–074008.
[19] U. Nwagwu, Flux growth and characteristics of cubic boron phosphide, Kansas State Universty, 2013. Master of Science Thesis.
[20] J.M. Soler, E. Artacho, J.D. Gale, A. García, J. Junquera, P. Ordejón, D. Sánchez-Portal, The SIESTA method for ab initio order-N materials simulation, J. Phys. Condens. Matter. 14 (2002) 2745–2779.
[21] N. Troullier, J.L. Martins, Efficient pseudopotentials for plane-wave calculations, Phys. Rev. B. 43 (1993) 1993–2006.
[22] C. Lee, W. Yang, R.G. Parr, Development of the Colic-Salvetti correlation-energy into a functional of the electron density, Phys. Rev. B. 37 (1988) 785–789.
[23] A.D. Becke, Density-functional exchange-energy approximation with correct asymptotic behavior, Phys. Rev. A. 38 (1988) 3098–3100.
[24] M. Parrinello, A. Rahman, Polymorphic transitions in single crystals: a new molecular dynamics method, J. Appl. Phys. 52 (1981) 7182–7190.
[25] M. Durandurdu, Amorphous boron arsenide, J. Non. Cryst. Solids 524 (2019), 119656.
[26] R.G. Delaplane, T. Lundström, U. Dahlborg, W.S. Howells, A neutron diffraction study of amorphous boron, in: AIP Conf. Proc, AIP Publishing, 1991, pp. 241–244.
[27] R. Naslain, Crystal chemistry of boron and of some boron-rich phases; preparation of boron modifications, in: V.I. Matkovich (Ed.), Boron Refract. Borides, Springer Berlin Heidelberg, Berlin, Heidelberg, 1977, pp. 139–202.
[28] S. Krishnan, S. Ansell, J.J. Felten, K.J. Volin, D.L. Price, Structure of liquid boron, Phys. Rev. Lett. 81 (1998) 586–589.
[29] S.R. Elliott, J.C. Dore, E. Marseglia, The structure of amorphous phosphorus, Le J. Phys. Colloq. 46 (1985) 349–353.
[30] D. Hohl, R.O. Jones, Amorphous phosphorus: a cluster-network model, Phys. Rev. B. 45 (1992) 8995–9005.

[31] H. Thurn, H. Krebs, Über struktur und eigenschaften der halbmetalle. XXll. Die kristallstruktur des Hittorfschen phosphors, Acta Cryst. B25 (1969) 125–135.
[32] T.A. Halgren, W.N. Lipscomb, Self-consistent-field wavefunctions for complex molecules. the approximation of partial retention of diatomic differential overlap, J. Chem. Phys. (1973) 1569–1591.
[33] S.K. Estreicher, C.H. Chu, D.S. Marynick, Equilibrium structures of neutral interstitial hydrogen in zinc-blende BN and BP, Phys. Rev. B. 40 (1989) 5739–5744.
[34] R.J. Archer, R.Y. Koyama, E.E. Loebner, L.R. Lucas, Optical absorbtion, electroluminescence, and the band GAP of BP, Phys. Rev. Lett. 12 (1964) 538–540.
[35] V.I.A. Fomichev, I.I. Zhukova, Investigation of the energy band structure of boron phosphide by ultra-soft X-ray spectroscopy, J. Phys. Chem. Solids 29 (1968) 1025–1032.
[36] Z.Y. Jiao, S.H. Ma, Y.L. Guo, Simulation of optical function for phosphide crystals following the DFT band structure calculations, Comput. Theor. Chem. 970 (2011) 79–84.
[37] P. Rodriguez-Hernandez, M. Gonzalez-Diaz, A. Munoz, Electronic and structural properties of cubic BN and BP, Phys. Rev. B. 51 (1995) 14705–14708.
[38] A. Zaoui, S. Kacimi, A. Yakoubi, B. Abbar, B. Bouhafs, Optical properties of BP, BAs and BSb compounds under hydrostatic pressure, Phys. B Condens. Matter. 367 (2005) 195–204.
[39] W.R.L. Lambrecht, B. Segall, Electronic structure and bonding at SiC/A1N and SiC/BP interfaces, Phys. Rev. B. 43 (1991) 7070–7085.
[40] S.Q. Wang, H.Q. Ye, A plane-wave pseudopotential study on III-V zinc-blende and wurtzite semiconductors under pressure, J. Phys. Condens. Matter. 14 (2002) 9579–9587.
[41] R.M. Wentzcovitch, K.J. Chang, M.L. Cohen, Electronic and structural properties of BN and BP, Phys. Rev. B. 34 (1986) 1071–1079.
[42] M.P. Surh, S.G. Louie, M.L. Cohen, Quasiparticle energies for cubic BN, BP, and BAs, Phys. Rev. B. 43 (1991) 9126–9132.
[43] A. Abdiche, R. Baghdad, R. Khenata, R. Riane, Y. Al-Douri, M. Guemou, S. Bin-Omran, Structural and electronic properties of zinc blende BxAl1-xNyP1-y quaternary alloys via firrst-principle calculations, Phys. B Condens. Matter. 407 (2012) 426–432.
[44] M. Merabet, D. Rached, R. Khenata, S. Benalia, B. Abidri, N. Bettahar, S. Bin Omran, Electronic structure of (BP)n/(BAs)n (0 0 1) superlattices, Phys. B Condens. Matter. 406 (2011) 3247–3255.
[45] R. Ahmed, A. Fazal, S.J. Hashemifar, H. Akbarzadeh, First-principles study of the structural and electronic properties of III-phosphides, Phys. B Condens. Matter. 403 (2008) 1876–1881.
[46] A. Zaoui, F.E.H. Hassan, Full potential linearized augmented plane wave calculations of structural and electronic properties of BN, BP, BAs and BSb, J. Phys. Condens. Matter. 13 (2001) 253–262.
[47] B. Cai, D.A. Drabold, Properties of amorphous GaN from first-principles simulations, Phys. Rev. B. 84 (2011) 075216.
[48] D. Udron, A.M. Flank, A. Gheorghiu, P. Lagarde, M.L. Theye, Evidence of chemical disorder in amorphous GaP, Phys. B. 158 (1989) 625–626.
[49] C.J. Glover, M.C. Ridgway, K.M. Yu, G.J. Foran, T.W. Lee, Y. Moon, E. Yoon, Structural characterization of amorphized InP: evidence for chemical disorder, Appl. Phys. Lett. 74 (1999) 1713–1715.